Supporting Information

X-ray Transparent Microfluidic Platforms for Membrane Protein Crystallization with Microseeds

J. M. Schieferstein,[a]† A. S. Pawate,[a]† M. J. Varel,[a] S. Guha,[a] I. Astrauskaite,[b] R. B. Gennis[b] and P. J. A. Kenis*[a]

[1]Department of Chemical & Biomolecular Engineering, University of Illinois at Urbana-Champaign, Urbana, Illinois 61801, USA
[2]Department of Biochemistry, University of Illinois at Urbana-Champaign, Urbana, IL 61801

Fabrication of microfluidic chips

SU-8 on silicon masters

Photoresist-on-silicon masters were fabricated through photolithography with SU8-2050 photoresist (Microchem) for patterns with vertical heights of 50 µm. Photomasks were designed using Adobe Illustrator and printed by Fineline Imaging at 10,000 dpi (Fig. S1). For designs with dense features and high aspect ratios, a 350 nm long pass filter (Omega Optical) was used. All photoresist-on-silicon masters were treated with silane vapors (Gelest, tridecafluoro-1,1,2,2-tetrahydrooctyl trichlorosilane) in a vacuum chamber for 4 h for easy release of PDMS replicas.

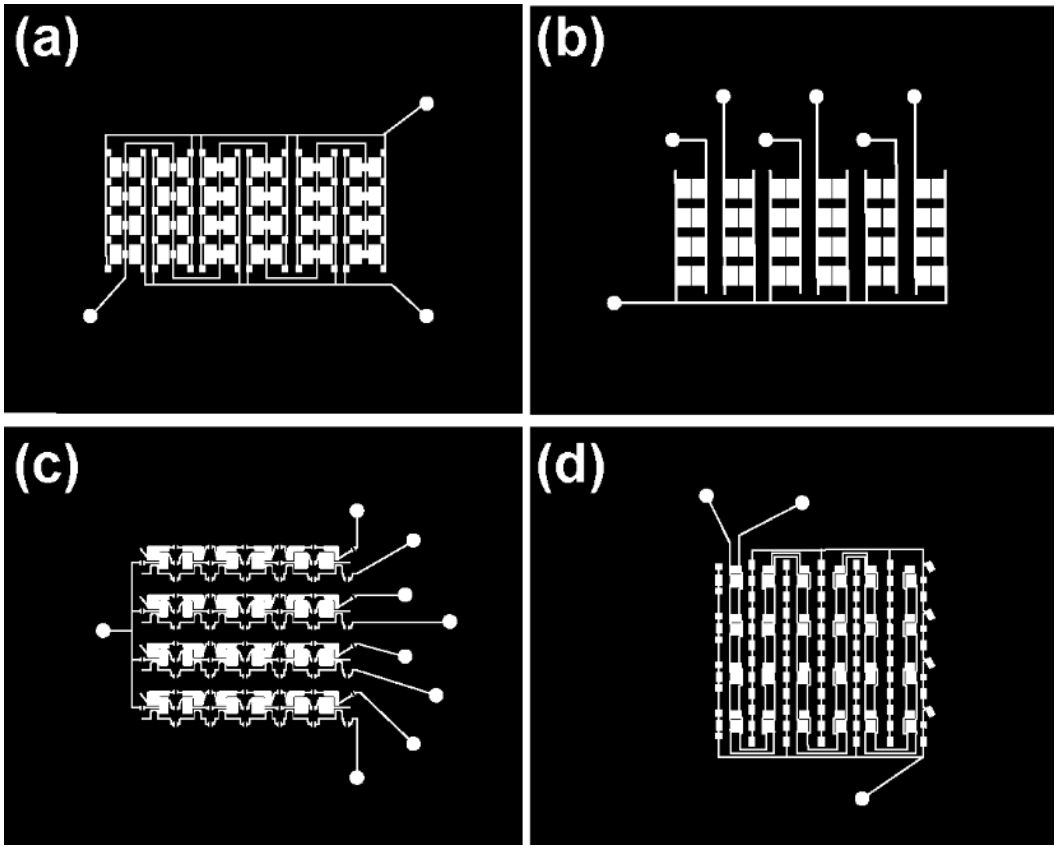

Figure S1. Photomasks for the two microseeding chips. **(a,b)** Control layer and fluid layer for the chip for simplified microseeding discussed in part A (Fig. 2). **(c,d)** Fluid layer and control layer masks for microseed screening chips discussed in part B (Fig. 3). Photomasks were printed at 10,000 dpi on a Mylar transparency film (Fineline Imaging).

Thin device for microseeding crystallization

Details of this procedure (Fig. S2) are adapted from previous publications (Guha *et al.,* Sens. Actuator B 2012; Schieferstein *et al.,* Biomicrofluidics 2017). Microfluidic devices were composed of 4 layers: an unpatterned COC top layer and two patterned PDMS layers to make the irreversibly bonded three-layer assembly (TLA) and the patterned COC substrate layer. To fabricate the three-layer assembly, first 60 µm of 5:1 PDMS was spin coated on the control layer master (10 µm thicker than the SU8 features) and baked at 90°C for 2 min. The coated wafer and an unpatterned 2-mil COC layer were then placed in a plasma cleaner (Harrick, PDC-001). After treatment at 500–700 mTorr for 1 min, the two layers were brought into conformal contact and heated at 70°C for 10 min to form an irreversibly bonded COC–PDMS assembly. Next, 60 µm of 15:1 PDMS was spin-coated on the fluid layer master and baked for 10 min at 90°C. The COC–PDMS assembly was released from the control layer master, aligned over the PDMS coated fluid layer master, brought into conformal contact, and baked at 65°C for 2 h to form the irreversibly bonded TLA. The TLA was released from the silicon wafer, inlet holes for fluid and vacuum were drilled with a 200 µm drill bit (McMaster-Carr) and reversibly bonded to a lipid-filled hot-pressed

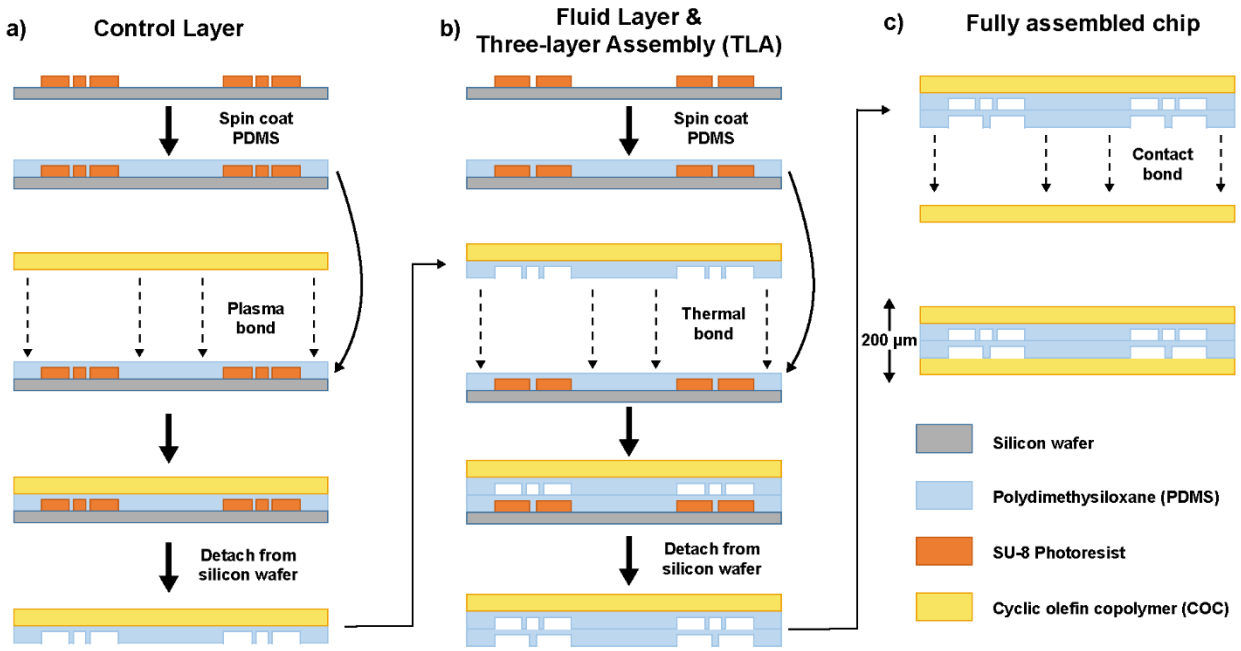

Figure S2. Fabrication scheme for multilayer COC/PDMS chips. **(a)** A 60 µm thick film of 5:1 (monomer-to-crosslinker) PDMS is spin coated onto a control layer SU-8 patterned silicon master (features from Fig. S1) and cured. A thin sheet of COC is bonded to the backside, and used to facilitate lift-off, resulting in a COC/PDMS control layer. **(b)** A 60 µm thick film of 15:1 PDMS is spin coated onto a fluid layer SU-8 silicon master and cured. Next, the COC/PDMS control layer from **(a)** is aligned over the cured fluid layer and then cured together. After at least two hours, the fluid layer and control layer (COC/PDMS/PDMS) three-layer assembly (TLA) are removed from the silicon and then **(c)** sealed by a contact adhesion bond to a flat layer of COC.

COC substrate to complete assembly of the chip.

Simulation of on-chip mixing time

Simulations were performed to determine mixing times and final concentrations for the microseed screening platform (Fig. S3)

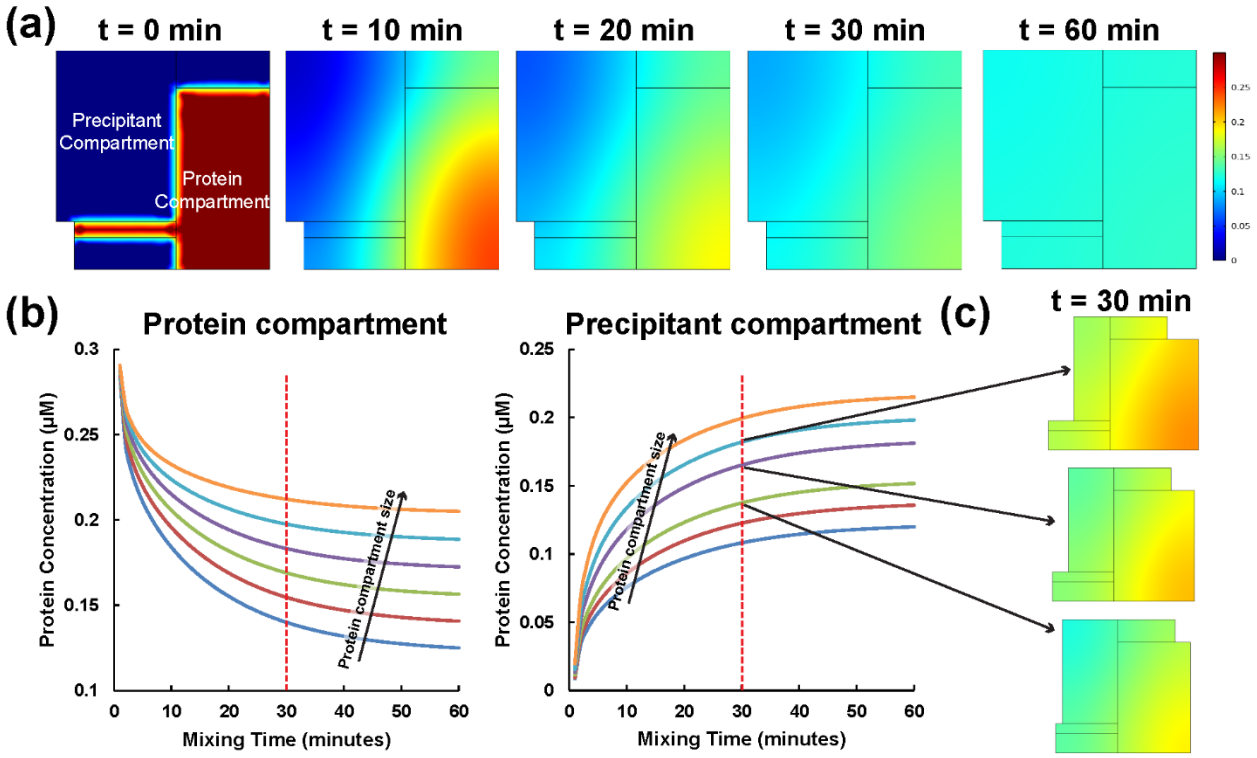

Figure S3. Computational fluid dynamics simulations using COMSOL to determine mixing times and final concentrations. **(a)** Snapshots of protein concentrations over a 60-minute free interface diffusion simulation. **(b)** Integral concentrations at each time point in the protein compartment (left) and the precipitant compartment (right) for each of 6 different compartment sizes. On-chip experiments ran for 30 minutes, indicated by the red dashed line. **(c)** Concentration surfaces of three intermediate-sized crystallization wells after 30 minutes.

Measurement of crystal aspect ratios

Cytochrome *bo*$_3$ oxidase crystals were measured at each protein-precipitant concentration (Fig. S4) and

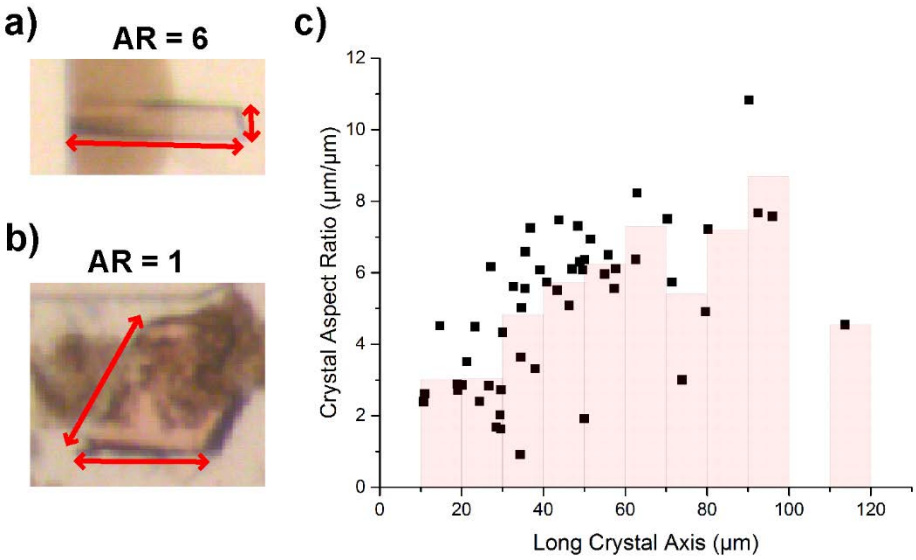

Figure S4. Measurement of cytochrome *bo*$_3$ oxidase crystal growth after 14 days. **(a)** At the 14-day mark, a picture was taken of every crystallization well such that every crystal grown was visible. Each image was analyzed manually using ImageJ – the length and width of each crystal was measured and assigned to the crystallization conditions at which it was grown. **(b)** Visualization of all crystal measurements, each point represents a single crystallization condition, while the red bar graph tracks the binned average. With some exceptions, longer crystals had larger aspect ratios. Long crystals with small aspect ratios are attractive targets for crystallography, as they are usually large in all dimensions and are expected to diffract well

used to construct phase diagrams (Fig. 5).

Crystal characteristics in different regions of supersaturation

For each supersaturation region highlighted on the phase diagram, crystal aspect ratios and diffraction resolutions were grouped and averaged (Fig. S5). Notably, the standard errors are small especially for diffraction quality in region 1 and aspect ratio for regions 1 and 2. This indicates that crystals that diffract to ~10.5 Å can be reliably grown, or that crystal populations of either thin needles or larger 3-dimensional can be grown by choice of supersaturation condition.

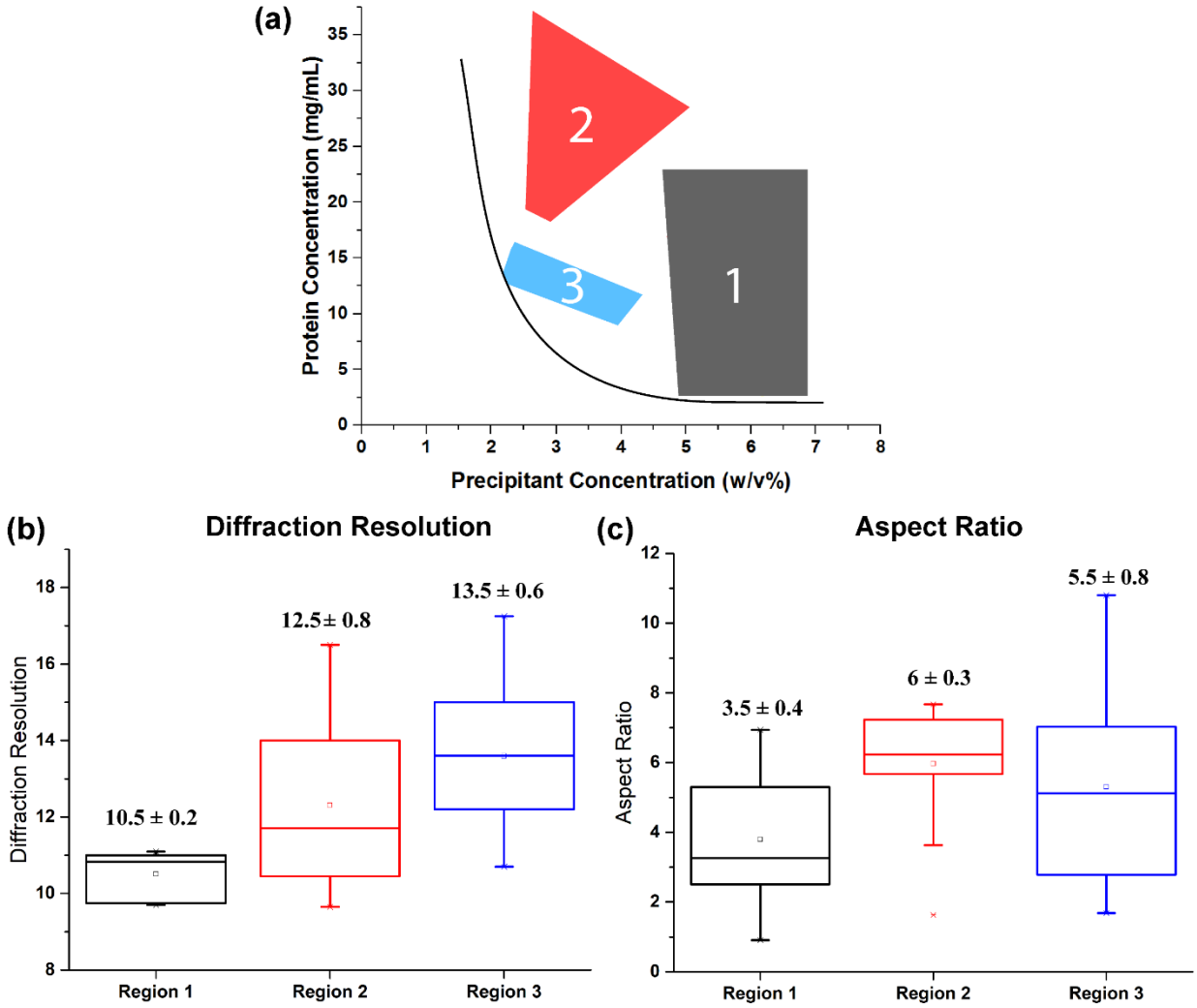

Figure S5. Crystallization characteristics in each supersaturation region on the phase diagram. **(a)** Three different groups of crystallization conditions shown on the cyt bo_3 phase diagram. **(b,c)** Box-and-whisker plots for each supersaturation region (defined in **(a)**) showing the distribution, range, and outliers for **(b)** diffraction resolution and **(c)** aspect ratio. The mean value and standard error are reported for each population.

Comparison of on-chip and off-chip crystallographic data for PYP

In situ diffraction data from room temperature experiments were compared to crystals grown and analyzed with traditional benchtop methods (Borgstahl, G.E. *et al.,* Biochemistry **1995**, *34*, 6278-6287).

Table S1
Crystallographic data[a] comparison for PYP

	On-chip	**Borgstahl *et al.* (PDB: 2PHY)**
Unit cell dimensions (Å)	a = b = 66.76 c = 40.89	a = b = 66.9 c = 40.8
Space group	$P6_3$	$P6_3$
Resolution (Å)	1.32	1.4
No. unique reflections	24,364	19,756
Completeness[b]	99.9% (98.4%)	92.7 (81.4)
Redundancy[b]	7.9 (6.7)	3.3 (-)
Mosaicity (deg.)	0.02 - 0.54	-
I/σ[b]	11.1 (2.3)	13.8 (1.7)
R_{sym}[b]	0.111 (0.508)	0.04 (0.207)